FIBRES & TEXTILES in Eastern Europe

sciendo

FIBRES & TEXTILES in Eastern Europe

Research Article • DOI: 10.2478/ftee-2022-0017 FTEE • 151(3) • 2022 • 9–17

Coupling Characteristics of Needles and Backing Cloth During the Carpet Tufting Process

Yang Xu[1]*, Shuang Huang[2], Xiaowei Sheng[1], Sun Zhijun[1]

[1] College of Mechanical Engineering, Donghua University, No 2999 North Renmin Road, Songjiang, Shanghai 201620, P.R, China
[2] School of Mechanical and Automotive Engineering, Shanghai University of Engineering Science, 333 Longteng Road, Songjiang, Shanghai, 201620, P.R. China
* Corresponding author. E-mail: xuyang@dhu.edu.cn

Abstract
Focusing on the needle and backing cloth on a tufting machine type DHG801D-200, a finite element model was built using ABAQUS/Explicit software. The tufting processes, in which the individual tufting needles and 1/10 needle modules puncture the polypropylene woven and nonwoven fabrics (hot-air bonded nonwoven and thermo-calender bonded nonwoven), were simulated, respectively. Finally, the needle forces were estimated, and the deformations and stress field distribution of the backing cloth at different times were analysed.

Keywords
tufted carpet, finite element model, needle force, deformation of backing cloth.

1. Introduction

During the carpet tufting process, the needle moves up and down under the exact cooperation of the knife and hook, and then the yarn is woven into the bottom of the woven fabric or nonwoven fabric [1, 2]. In this dynamic puncture process at high speed, the backing cloth undergoes elastic deformation, plastic deformation, and then it is damaged. Moreover, the strength of the needle also is gradually weakened under the alternating stress. Each damaged needle will affect the quality of the tufted carpet, the production efficiency of equipment, and the labour productivity of workers. Furthermore, the force on the needle and the deformation of the backing cloth not only affect the yarn tension fluctuation but also the important parameters of the structural optimisation design on tufting equipment. Therefore, study of the coupling characteristics of the needle and backing cloth is a very important part of the tufting process.

Currently, research of the needle penetrating force is focused on the sewing needle. Karl Gotlih [3] established a mathematical model for calculating the needle penetration force and provided improvement suggestions based on this model; Haghighat et al. [4, 5] predicted the needle penetration force in denim fabric by using an artificial neural network and multiple linear regression models. To investigate the feasibility of measurement of the penetration force in real time, Carvalho et. al [6] measured the force when the needle pierced into and pulled out from the backing cloth, Lomov [7] proposed an algorithm to compute the maximum needle penetration force and simulated the deformation of woven material. Mallet et. al [8] simulated the needle piercing process to calculate the sewing forces as well as fabric deformation using the finite element model. However, the puncture objects of a tufting needle are polypropylene woven and nonwoven fabrics, while the puncture objects of a sewing needle are knitted fabrics, which makes a big difference and cannot be completely copied.

There are three methods to analyse the coupling characteristics of the needle and backing cloth: the theoretical analysis method, the experimental test method, and the finite element method. The finite element method has a great advantage in calculating the dynamic puncture force with high speed, as well as the stress and strain, which change over time [9-13]. Therefore, focusing on the needle and backing cloth on a tufting machine type DHG801D-200, the puncture processes of individual tufting needles and 1/10 needle modules in polypropylene woven and nonwoven fabrics were simulated, respectively, and the needle forces and fabric deformation were analysed.

2. Models of needle and backing cloth

In the finite element analysis of the carpet tufting process, the two parts mainly related are the tufting needle and backing cloth, with the latter containing polypropylene woven fabrics and nonwoven fabrics.

2.1. Model of needle

The tufting needle is one of the most important parts on a tufting machine, whose specification and quality directly affect the appearance and weaving precision of tufting carpet. Taking the 1/10 needle modules produced by Groz-Beckert company as the research object, the needle modules have ten needles in one inch. The parameters of the tufting needle are listed in Table 1. According to the actual size of the needle, a model of the needle was built in Solidworks software. The models of individual tufting needles and 1/10 needle modules are shown in Figure 1.

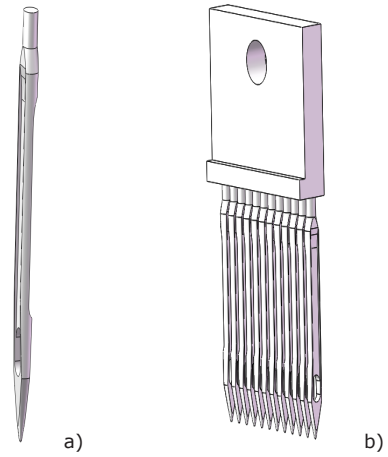

Fig. 1. Models of tufting needles. a) Individual tufting needle; b) 1/10 needle module

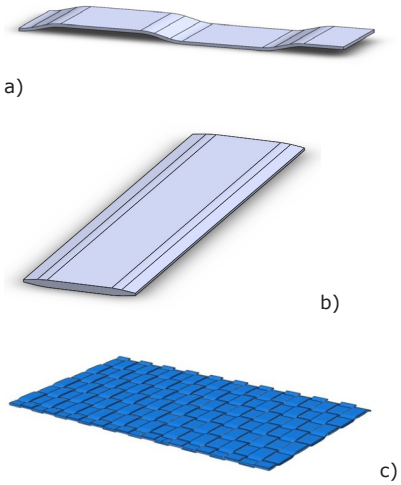

Fig. 2. Model of polypropylene woven fabric a) model of warp, b) model of weft, c) complete model

2.2. Model of backing cloth

In the tufting process, the yarn is woven into the backing cloth. And the backing cloth is related to the tearing strength of the carpet. Thus, the parameters of strength, elongation and density of the backing cloth yarns have a great influence on the quality of tufting carpet. At present, the majority of tufting carpet backing cloths is polypropylene woven and nonwoven fabric. In addition, the nonwoven fabrics commonly used for tufting carpet are hot-air bonded or thermo-calender bonded nonwovens.

2.2.1. Model of polypropylene woven fabric

Before modelling, several assumptions were made: (1) neglecting small differences in the mechanical properties of different yarn segments; the yarn of the backing cloth is regarded as a uniform entity; (2) the yarn is an isotropic elastic material, and the differences between the yarns are ignored; (3) yarns are tightly interwoven. and there is no gap between them .

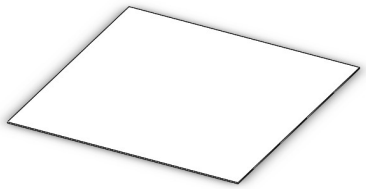

Fig. 3. Model of the nonwoven fabric

The object analysed was a backing cloth of 0.24 mm thickness, 24 mm length and 12 mm width. For the warp the elastic modulus was 55 MPa, the linear density - 57.87 tex, and the Poisson ratio - 0.41; for the weft the elastic modulus was 140 MPa, the linear density - 98.44 tex, and the Poisson ratio was also 0.41. Mechanical properties of the polypropylene woven fabric are listed in Table 2. Using Solidworks software, a 3D model of the polypropylene woven fabric was constructed, shown in Figure 2. During the modelling process, a warp model is formed by scanning along a specific route based on the section feature, a weft model by stretching, and then the warp and weft are assembled to form a geometric model of the polypropylene woven fabric.

2.2.2. Model of nonwoven fabric

Nonwoven fabric is made up of a fiber network structure which is oriented or randomly arranged using a mechanical, thermal or chemical method. Because of the discontinuity of the structure, the mechanical properties of nonwoven fabric have highly nonlinear characteristics. In this paper, the nonwoven fabric is regarded as an integrated whole (Figure 3). Through experimental tests, the mechanical properties of hot-air bonded and thermo-calender bonded nonwovens were measured, respectively, listed in Table 3 and Table 4. In Table 4, E_{11}, E_{22} and E_{33} are the Young's moduli of the x, y z direction respectively, G_{12}. G_{23} and G_{31} - the shear moduli of the XY plane, YZ plane and ZX plane, respectively and v_{12}, v_{23} and v_{13} are the Poisson's ratios of the XY plane, YZ plane and ZX plane, respectively. When using the finite element method, the object analysed was nonwoven fabric of 80mm length and 80mm width.

Material	Gauge [in]	Density [g.cm-3]	Length [mm]	Thickness [mm]	Elastic modulus [MPa]	Poisson ratio
Steel	0.10	7.8	36	3	2700	0.28

Table 1. Parameters of tufting needle

Yarn	Stress [MPa]	Strain	Fracture work [mJ]
Warp	249.5	0.056	1400.00
Weft	243.0	0.081	1291.31

Table 2. Mechanical properties of polypropylene woven fabric

Backing cloth	Fiber fineness [dtex]	Density [g/m2]	Thickness [mm]	Length [mm]	Width [mm]
Hot-air bonded nonwoven	1.56	110	0.24	30	26
Thermo-calender bonded nonwoven	1.56	65	0.35	30	26

Table 3. Specification parameters of nonwoven fabrics

3. Finite element simulation

Commercial finite element software, ABAQUS/Explicit [14], was employed for simulation of the tufting process. The deformation of the backing cloth and the penetration force were analysed.

Backing cloth	E_{11} [MPa]	E_{22} [MPa]	E_{33} [MPa]	G_{12} [MPa]	G_{23} [MPa]	G_{31} [MPa]	ν_{12}	ν_{23}	ν_{13}
Hot-air bonded nonwoven	357.59	140.04	9.80	121.98	50.01	4.86	0.41	0.41	0.41
Thermo-calender bonded nonwoven	126.75	94.56	10.00	87.88	49.66	4.86	0.41	0.41	0.41

Table 4. Mechanical properties of nonwoven fabrics

When using the finite element method, setting up the right parameters, such as the material properties, contact and boundary conditions, are the key to get the correct results. The material properties of the needle and backing cloth are listed in Tables 1-4. The contact between the needle and backing cloth was defined as "general contact". The friction coefficient between the needle and backing cloth was set to 0.5, and that between the warp and weft in polypropylene woven fabric to 0.1 [15, 16]. Since the stiffness of the needle is much larger than that of the backing cloth and the deformation of the needle can be ignored during the penetration, the needle can be regarded as a rigid body. The damage of the backing cloth is determined both by the plastic criterion and the shear criterion in the finite element model. Once a damage criterion is reached, the material stiffness will be damaged according to the damage development rule.

3.1. Boundary conditions and load

For saving computing time, and due to the symmetry of the model, only a 1/2 part of the tufting needle and backing cloth was analysed in the finite element calculation. In the initial analysis step, a fixed constraint was applied to the other three boundaries of the bottom cloth. And symmetry constraints were applied to the reference points of the needle and backing cloth . Since the needle can only move up and down in one direction, the other five degrees of freedom of the needle are constrained at its reference point. As seen from the reference [17], a speed curve of the tufting needle can be obtained using ADAMS software, and the velocity equation of the needle can be written as:

$$V = -1000\cos\frac{\pi t}{30} \quad (1)$$

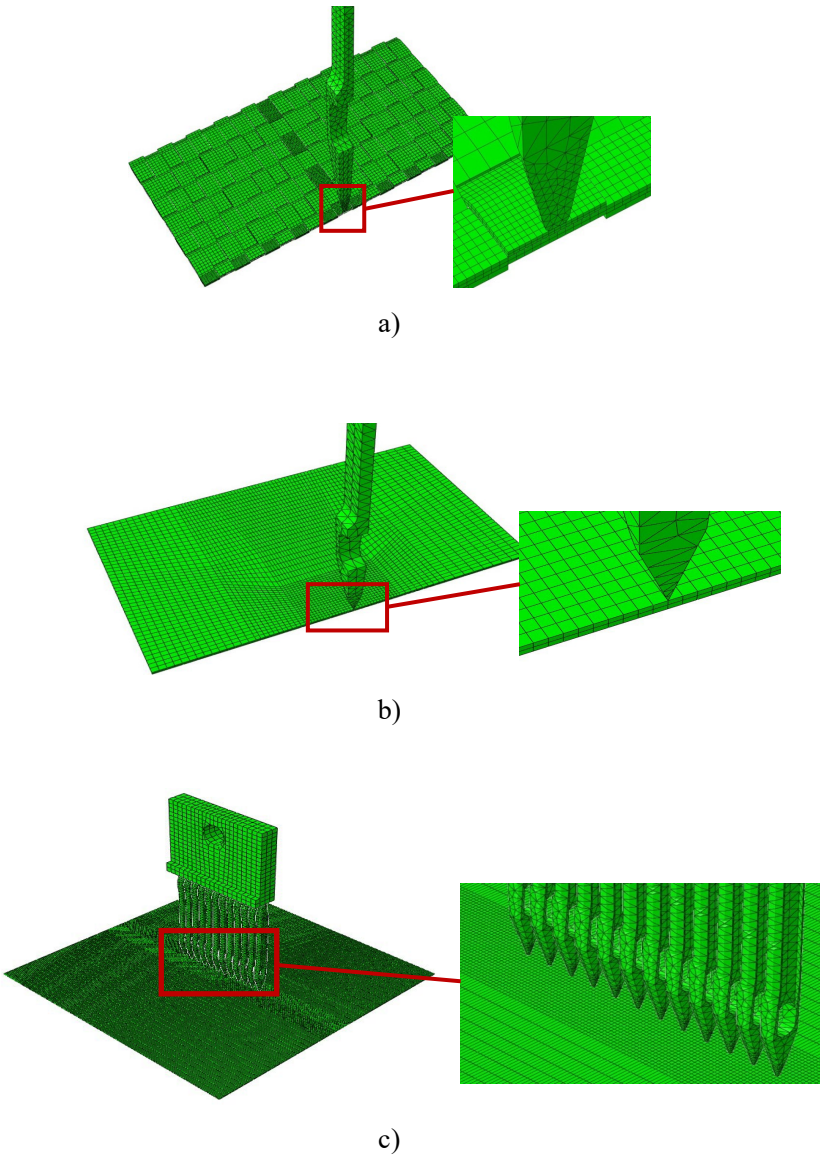

Fig. 4. Meshing in the finite element model a) single needle and polypropylene woven fabric, b) single needle and nonwoven fabric, c) 1/10 needle modules and nonwoven fabric

3.2. Meshing

The quality of the element meshing is very significant to the accuracy and effectiveness of the finite element model calculation results. To improve the quality of meshing, topology optimisation of the backing cloth was carried out prior to dividing the mesh, and the adjacent plane was merged, the sharp geometric angle was reduced. The needle was meshed using C3D10M elements, and the backing cloth using C3D8R elements. To improve the calculation accuracy, a graded mesh was thus created, where the region in the contact parts between the needle and backing cloth was more finely meshed, as shown in Figure 4.

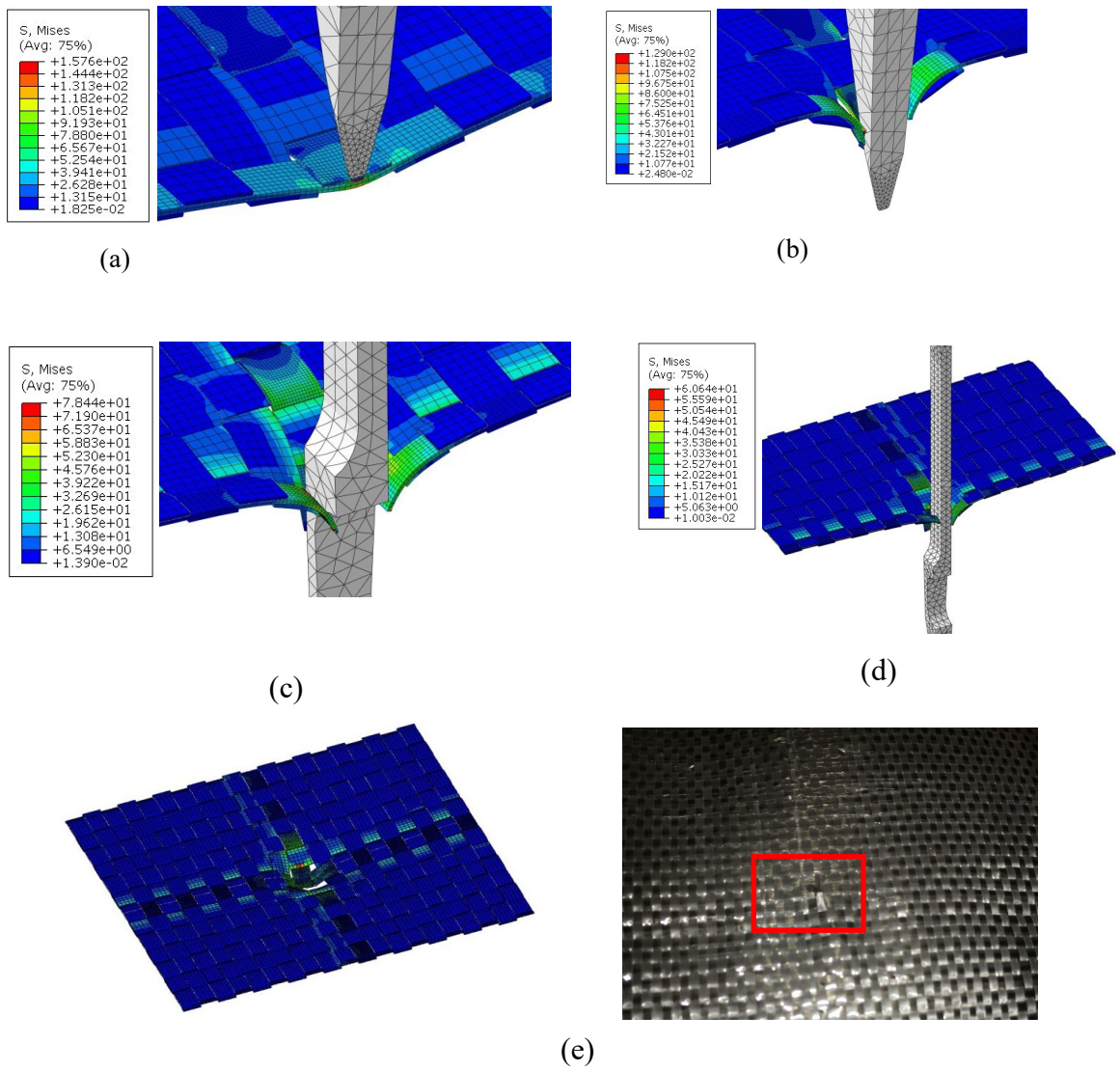

Fig. 5. Deformation of the polypropylene woven fabric at time t: a) t=1.5ms, b) t=3ms, c) t=11.25ms, d) t=15ms, e) hole in fabric in the finite element model and in the actual backing cloth (t=15ms)

4. Results and discussion

During the tufting process, the coupling characteristics of the needle and backing cloth are affected by the speed of the needle and the material of the backing cloth. Hence, according to these different conditions, deformations of the backing cloth and penetration force were analysed in the finite element model.

4.1. Deformation of polypropylene woven fabric

The deformations of the polypropylene woven fabric were obtained at different times, as shown in Figure 5(a-e). As seen in the simulation results, at time t=1.5ms, the force of the backing cloth gradually decreases from the contact point to the outer parts, as shown in Figure 5a. Under the action of the needle, stress concentration occurred at the contact parts, and the value of the maximum stress was 150 MPa. At t=3ms, the elements in contact between the needle and backing cloth were damaged. The elements around the damaged parts caused the strain, shown in Figure 5b. In Figure 5c, the upper boundary of the pinhole was exposed to the back of the cloth, and the value of maximum stress increased to 78 MPa. At t=15ms, the needle completely penetrated through the backing cloth, as shown in Figure 5d. As seen from Figure 5a-e, the results of the finite element simulation are consistent with the actual deformation of the backing cloth, which shows that the finite element model of the tufting penetration process is basically correct.

4.2. Deformation of nonwoven fabric and needle penetration force

4.2.1. Deformation of hot-air bonded nonwoven

The deformations of the hot-air bonded nonwoven assessed at different times are shown in Figure 6a-g. As seen in the simulation results, at the time of 13ms,

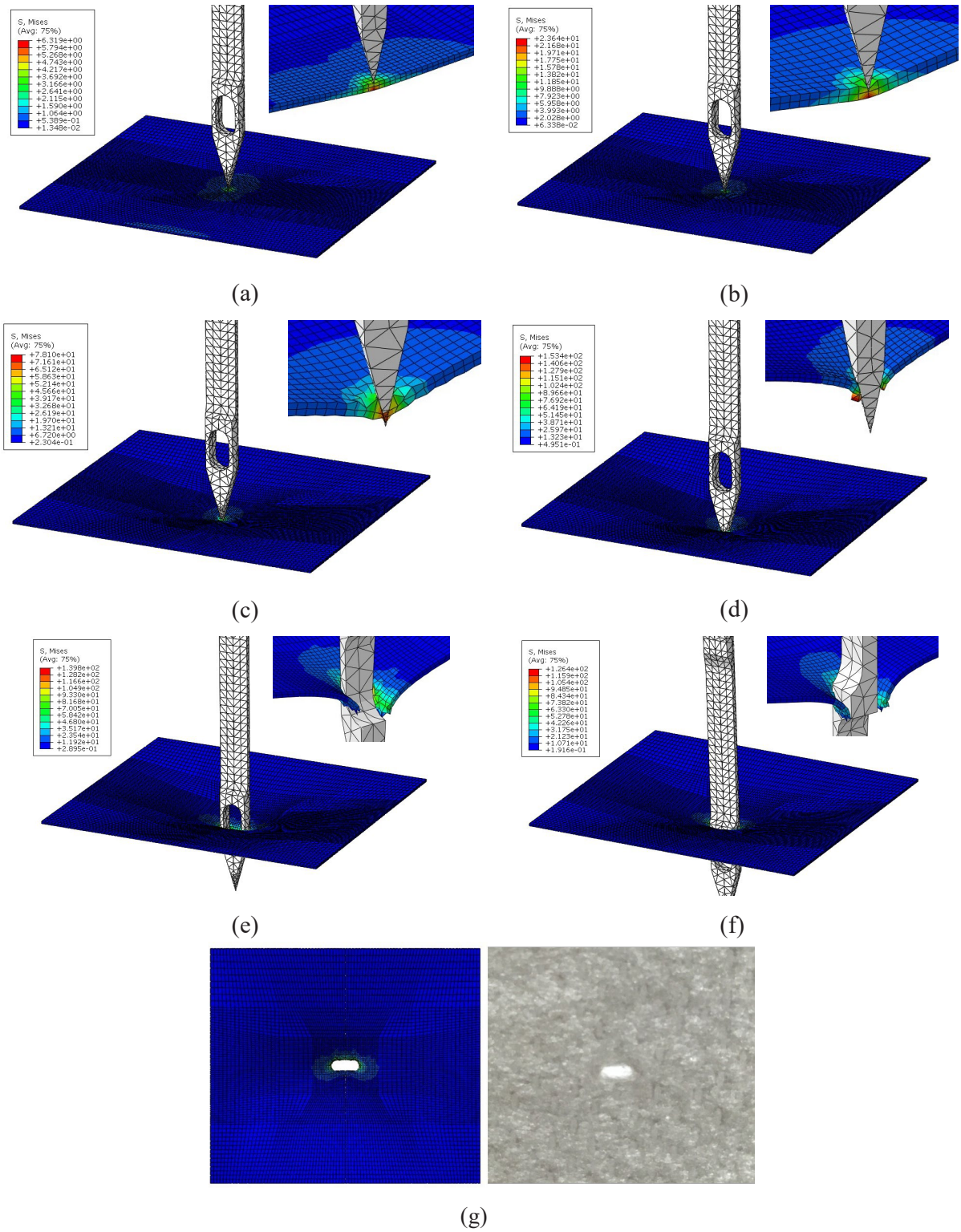

Fig. 6. Deformation of the hot-air bonded nonwoven at time t: a) t=0.65ms, b) t=1.3ms, c) t=2.6ms, d) t=4.55ms, e) t=9.75ms, f) t=13ms, g) hole in fabric in the finite element model and in the actual backing cloth (t=13ms)

the needle completely penetrated through the backing cloth. From Figure 8g, the deformation of the hole in the fabric in the finite element model agrees with the actual hole shape of the backing cloth.

4.2.2. Deformation of thermo-calender bonded nonwoven

Deformations of the thermo-calender bonded nonwoven obtained at different times are shown in Figures 7a-e. As seen in the simulation results, at a time of 15ms, the needle completely penetrated through the backing cloth.

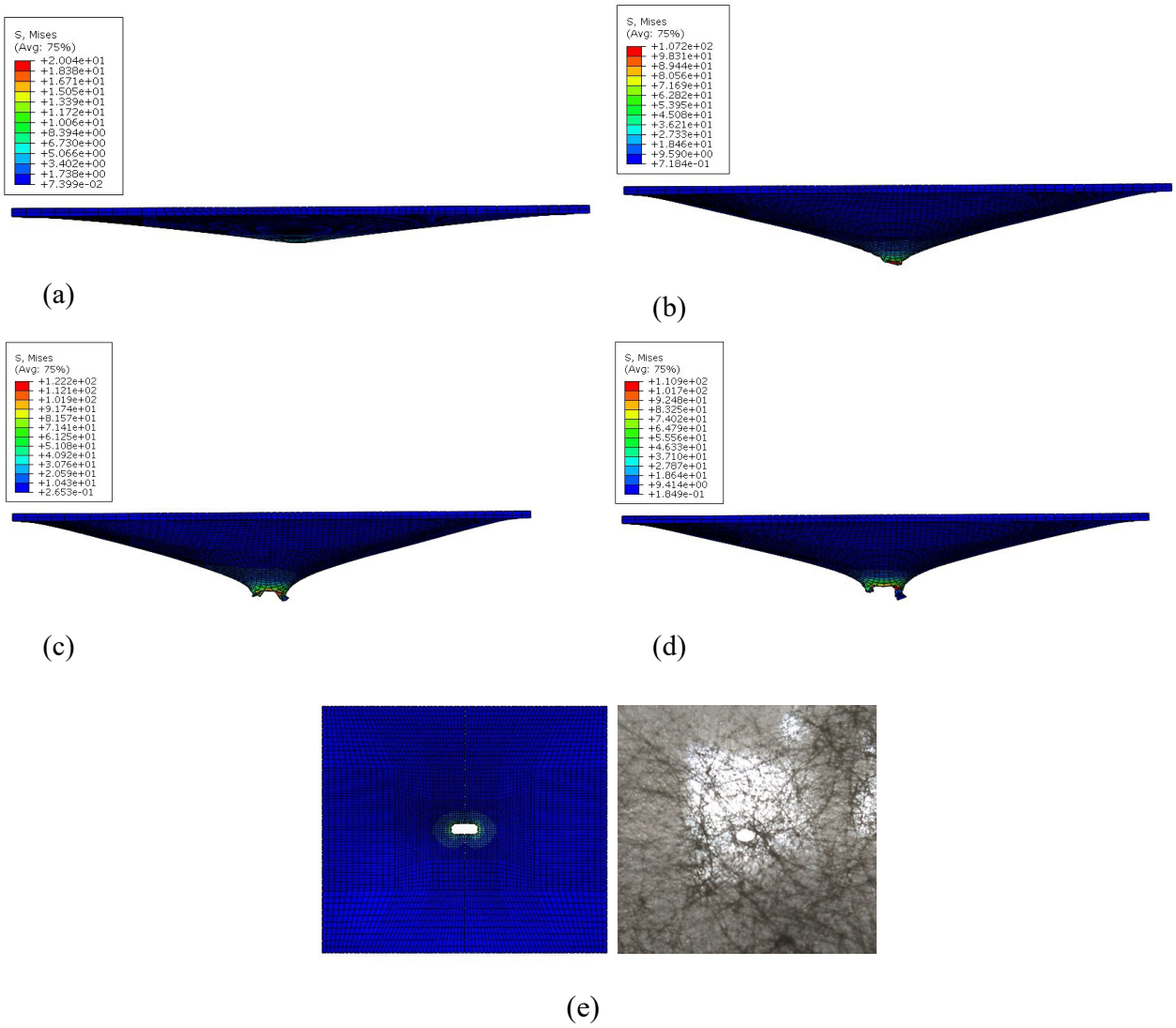

Fig. 7. Deformation of thermo-calender bonded nonwoven at time t: a) t=1.5ms, b) t=4.5ms, c) t=9ms, d) t=15ms, e) hole in fabric in the finite element model and the actual backing cloth (t=15ms)

4.2.3. Forces of needle and backing cloth

(1) Force of needle

Curves of the needle forces over time are shown in Figure 8. When the needle punctures the hot-air bonded nonwoven and does not pierce the backing cloth, the contact parts of the backing cloth undergo elastic deformation, the needle force increases slowly, and then the contact of the backing cloth experiences plastic deformation, and the needle force increases rapidly. At a time of 4ms, the backing cloth is damaged, and the needle force reaches 9 N, which mainly comes from the friction and resistance of the backing cloth. When the needle pierces into the backing cloth completely, the needle force decreases to 6 N, which mainly comes from the friction of the needle and backing cloth.

When the needle starts to puncture the nonwoven, at the stage of elastic and plastic deformation, the force is basically the same for both thermo-calender bonded nonwoven and hot-air bonded nonwoven. However, when the backing cloth is already damaged, the needle force is bigger for thermo-calender bonded nonwoven than for hot-air bonded nonwoven. The force reaches 17 N, and the reason for the difference in the needle force is that the friction coefficients of the backing cloths are different.

To understand the influence of the needle speed on the needle force, the amplitude of the initial needle velocity was set to -2000 mm/s. Curves of the needle force at different speeds are shown in Figure 9. Comparing the two curves, as the speed becomes larger, the needle force decreases, and the impact force subjected to the needle is also smaller.

(2) Forces on backing cloth

The maximum stress of nodes in the backing cloth is shown in Figure 10. When the elastic and plastic deformation occur, the maximum stress increases rapidly. And the maximum stress remains stable when the backing cloth is damaged. As

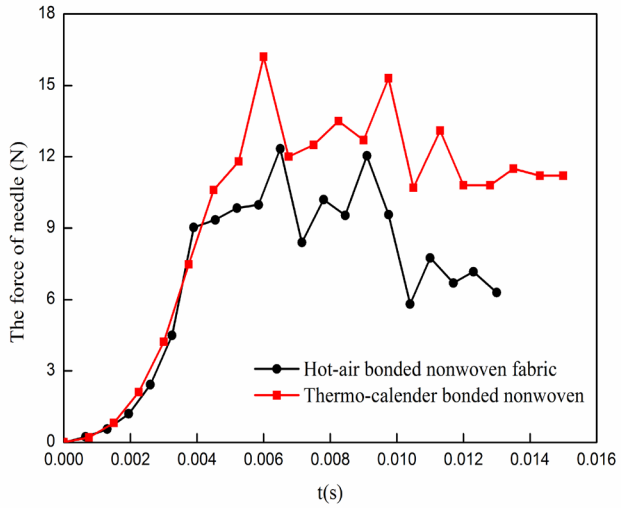

Fig. 8. Needle forces for different backing materials

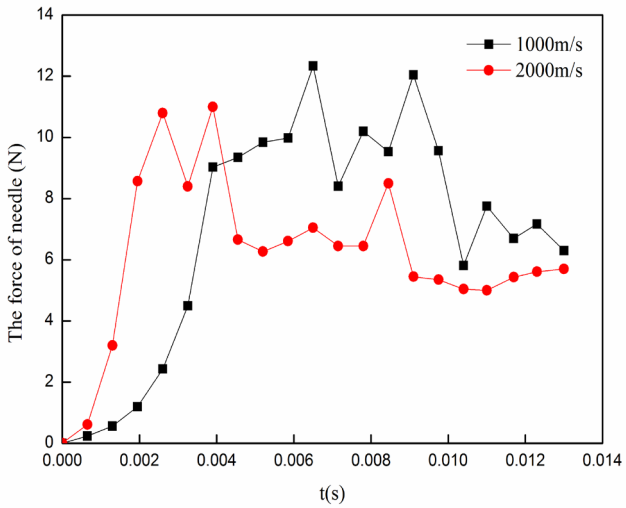

Fig. 9. Needle forces at different needle speeds

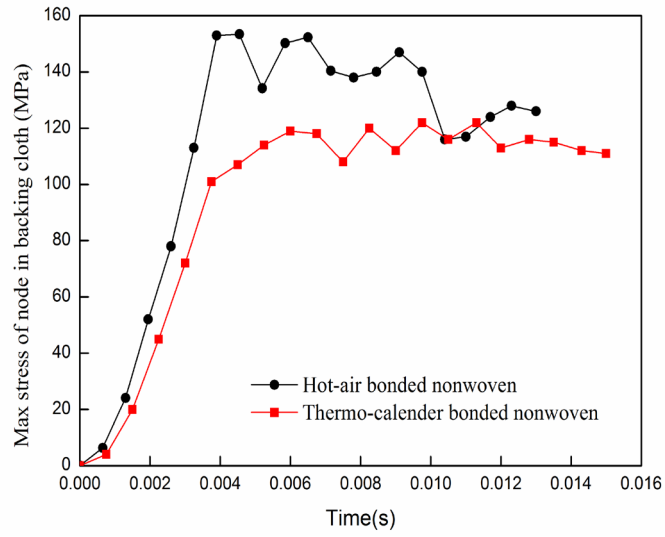

Fig. 10. Maximum stress of the node in the backing cloth

seen from Figures 10, the maximum stress of nodes in hot-air bonded nonwoven is bigger than that of nodes in thermo-calender bonded nonwoven. The peak value of the maximum stress in hot-air bonded nonwoven is 155 MPa, remaining at 120 MPa in the end. And finally the maximum stress in thermo-calender bonded nonwoven remains at 110 MPa.

4.2.4. Deformation of hot-air bonded nonwoven when punctured by 1/10 needle modules

The deformations of hot-air bonded nonwoven punctured by 1/10 needle modules are shown in Figures 11a-e, and Figure 11g illustrates the actual shape of the hot-air bonded nonwoven. As seen from the Von Mises stress cloud, under the condition of the ends of the four sides of the backing cloth being fixed, the two outermost needles in the modules pierce into the backing cloth first; consequently, the maximum stress occurs on the both sides of the backing cloth, which reached 10 MPa. At t=3.75ms, as shown in Figure 13c, all ten needles penetrated the backing cloth, the backing cloth showed plastic deformation, and the maximum stress of the node was larger than 154 MPa. At t=4.5ms (Figure 13d) the stress was larger than the fracture stress threshold, and the backing cloth was damaged. And at t=10ms the penetration process was completely finished.

5. Conclusion

A finite element model of the needle and backing cloth was built using ABAQUS/ Explicit, the tufting penetration process simulated, and then the needle force and the deformation of the backing cloth were analysed. The simulation results show the following :

(1) During the penetration process, the backing cloth undergoes elastic and plastic deformation before it is damaged, and the maximum stress increases rapidly. After the backing cloth is damaged, the maximum stress remains stable.

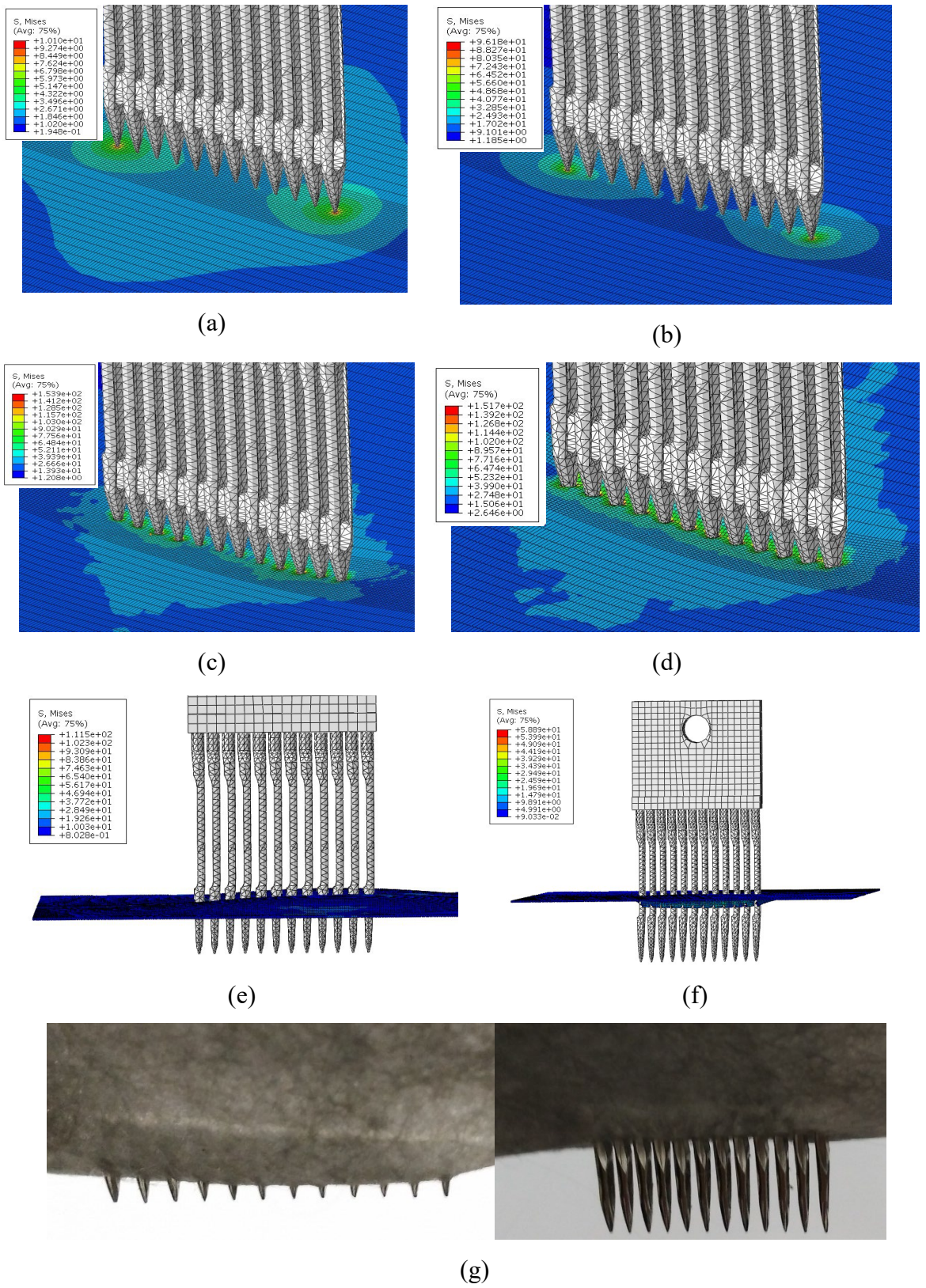

Fig. 11. Deformation of hot-air bonded nonwoven punctured by 1/10 needle modules at time t: a) t=0.75 ms, b) t=3 ms, c) t=3.75 ms, d) t=4.5 ms, e) t=5.25 ms, f) t=10 ms, g) actual backing cloth

(2) When the needle punctures thermo-calender bonded nonwoven, at the stage of elastic and plastic deformation, the force is basically the same as when puncturing hot-air bonded nonwoven. However, when the backing cloth is damaged, the needle force is bigger than that when puncturing hot-air bonded nonwoven.

(3) The maximum stress of nodes in hot-air bonded nonwoven is bigger than that of nodes in thermo-calender bonded nonwoven when the nonwoven is damaged.

The results of the finite element simulation are in good agreement with the actual deformation of the backing cloth, which shows that the finite element model of the needle puncture bottom cloth is basically correct. Therefore, it is reliable for getting data of the puncture force at different stages, which can provide a powerful reference for mechanical structure optimisation of a tufted carpet loom.

Funding

The authors gratefully acknowledge the financial support by the National Natural Science Foundation of China (51675094, 51905331) and Research and Key Projects of the Central University Fund (2232017A3-04).

References

1. Meng, Z., Sun, J. J., Zhou, T. Z., & Gu, S. H. (2008). Research on the Influence that Stop Position of Carpet Tufting Machine to Yarn Tension and the Method of Elimination Stop Mark. *Key Engineering Materials, 375-376*, 724-728.
2. Xue, S. (2003). *Machine-made carpet*. Beijing: Chemical Industry Press.
3. Gotlih, K. (1997). Sewing needle penetration force study. *International Journal of Clothing Science & Technology, 9* (3), 241-248.
4. Haghighat, E., Etrati, S. M., & Najar, S. S. (2013). Modeling of needle penetration force in denim fabric. *International Journal of Clothing Science & Technology, 25*(25), 361-379.
5. Haghighat, E., Etrati, S. M., Najar, S. S., & Shamsi, M. (2015). Theoretical prediction of the needle penetration force in denim fabric part 1: Yarn tensile extension component. *International Journal of Clothing Science & Technology, 27*(3), 397-416.
6. Carvalho, H., Rocha, A. M., & Monteiro, J. L. (2009). Measurement and analysis of needle penetration forces in industrial high-speed sewing machine. *Journal of the Textile Institute, 100*(4), 319-329.
7. Lomov, S. V. (1998). A predictive model for the penetration force of a woven fabric by a needle. *International Journal of Clothing Science & Technology, 10*(2), 91-103.
8. Mallet, E., & Du, R. (2013). Finite element analysis of sewing process. *International Journal of Clothing Science & Technology,* 11(11), 19-36.
9. Goda I., & Girardot J. (2021). Numerical modeling and analysis of the ballistic impact response of ceramic/composite targets and the influence of cohesive material parameters. *International Journal of Damage Mechanics*, 30(7):1079-1122.
10. Elias A., Laurin F., Kaminski M. & Gornet L.(2017). Experimental and numerical investigations of low energy/velocity impact damage generated in 3D woven composite with polymer matrix. *Composite Structures*, 159, 228-239.
11. Wu Z.Y., Zhang L. C., Ying Z.P., Ke J., & Hu X. D. (2020). Low-velocity impact performance of hybrid 3D carbon/glass woven orthogonal composite: Experiment and simulation. *Composites Part B: Engineering*, 196(1): 1-14.
12. Haque B. Z., & Gillespie J. W. (2021). Perforation mechanics of UHMWPE soft ballistic sub-laminate and soft ballistic armor pack: A finite element study. *Journal of thermoplastic composite materials,* 1-29 (online).
13. Zhang R., Qiang L. S., Han B., Zhao Z.Y., Zhang Q. C., Ni C. Y., & Lu T. J. (2020). Ballistic performance of uhmwpe laminated plates and uhmwpe encapsulated aluminum structures: numerical simulation. *Composite Structures,* 252: 112686.
14. Yiping Shi, Y. Z. (2006). *Finite element analysis of detailed examples using ABAQUS*. Beijing: Mechanical Engineering Press.
15. Wang, P., Ma, Q., & Sun, B. (2011). Finite element modelling of woven fabric tearing damage. *Textile Research Journal*, *81(12)*:1273-1286.
16. Masoumeh V., Stepan L., & Sayed A.(2010). Finite element modeling of a yarn pullout test for plain woven fabrics. *Textile Research Journal*, 80(10):892-903.
17. Ding, C. H., Zhang, S. P., & Sun, Y. Z. (2006). Kinematical analysis of the needle's driving mechanism within a carpet tufting machine. *Journal of Textile Research, 27*(5), 37-40.